

## P3.21 Annual Cycle of Cloud Forcing of Surface Radiation Budget

Anne C. Wilber<sup>1</sup>, G. Louis Smith<sup>2</sup>, Paul W. Stackhouse Jr.<sup>3</sup> and Shashi K. Gupta<sup>1</sup>

1. Analytical Services and Materials, Hampton, Virginia
2. National Institute of Aerospace, Hampton, Virginia
3. Langley Research Center, Hampton, Virginia

### 1. Introduction

The climate of the Earth is determined by its balance of radiation. The incoming and outgoing radiation fluxes are strongly modulated by clouds, which are not well understood. The Earth Radiation Budget Experiment (Barkstrom and Smith, 1986) provided data from which the effects of clouds on radiation at the top of the atmosphere (TOA) could be computed (Ramanathan, 1987). At TOA, clouds increase the reflected solar radiation, tending to cool the planet, and decrease the OLR, causing the planet to retain its heat (Ramanathan et al., 1989; Harrison et al., 1990). The effects of clouds on radiation fluxes are denoted cloud forcing. These shortwave and longwave forcings counter each other to various degrees, so that in the tropics the result is a near balance. Over mid and polar latitude oceans, cloud forcing at TOA results in large net loss of radiation. Here, there are large areas of stratus clouds and cloud systems associated with storms. These systems are sensitive to surface temperatures and vary strongly with the annual cycle. During winter, anticyclones form over the continents and move to the oceans during summer. This movement of major cloud systems causes large changes of surface radiation, which in turn drives the surface temperature and sensible and latent heat released to the atmosphere. Cloud forcing of surface radiation is thus an important feedback mechanism in atmospheric and oceanic processes.

The Surface Radiation Budget (SRB) Data Set (Whitlock et al., 1995) permits the investigation of the effects of clouds on the radiation budget at the surface of the Earth. This data set was developed in support of the Global Energy and Water Experiment and is based on data from the International Satellite Cloud Climatology Project ISCCP (Rossow and Schiffer, 1991; Schiffer and Rossow, 1983). It includes upward and downward shortwave and longwave radiation fluxes and the total radiation fluxes at the surface. The initial edition used a 2.5° latitude quasi-equal size grid over the globe and covered the period July 1983 through June 1991. The SRB data set has been upgraded by improvements of the algorithms used to compute the various components of radiation and refinement of the resolution (Stackhouse et al., 2004; Gupta et al., 2004). The SRB data set has recently been further upgraded to Release 2.5 (Cox et al., 2006) and covers a twenty-one-year period.

Darnell et al. (1992) used the earlier version of the SRB data set to study the seasonal variation of surface radiation budget. They presented maps of surface radiation components and latitudinal plots of zonal averages of the components of surface radiation. Gupta et al. (1993) investigated the cloud forcing for upward and downward shortwave, longwave and total radiation fluxes for July 1985 and January 1986. They demonstrated that the effect of clouds is to reduce downward shortwave (DSW) radiation and increase downward longwave (DLW) radiation. Clouds cool the surface in the summer hemisphere, where the reduction of DSW dominates, and warm the surface in the winter hemisphere, where the longwave radiation effect is greater. The global average total effect of cloud is to cool the

---

*Corresponding author address:*

Anne C. Wilber, NASA-Langley Research Center, MS 936, Hampton, VA 23681.  
email: [a.c.wilber@larc.nasa.gov](mailto:a.c.wilber@larc.nasa.gov)

surface. Gupta et al. (1999) compared the SRB data set to results from general circulation models and found that the models computed shortwave and longwave radiation which were 10 to 20  $\text{Wm}^{-2}$  greater than the SRB data set for global averages.

As the major cloud systems move during the year with the annual cycle of insolation, the effects of clouds on the downward and upward shortwave and longwave radiation fluxes at the surface vary also. There are a number of questions which arise concerning the annual cycle of surface radiation fluxes. The present paper uses the Release 2.5 of the GEWEX Surface Radiation Budget Data Set (Cox et al 2006) to investigate the annual cycles of cloud forcing of surface radiation components. In order to describe these annual cycles, a principal component analysis is used whereby the major cyclic effects are computed as time variations with maps revealing their geographical distributions. The advantage of this approach is that it represents the time and space variations with the minimum number of terms, which are determined by the data. The principal components are statistical descriptors rather than physical, but often have simple physical interpretations. Also, the principal components from the analysis of data can be compared with those from circulation model results as an objective technique for establishing the similarities and differences between the two in regard to time and space structure.

## 2. Data Set

The Release 2.5 Surface Radiation Budget data set includes the downward and upward reflected solar radiation flux at the surface, the upward longwave radiation flux at the surface and the longwave radiation flux from the atmosphere to the surface. These fluxes are provided on a  $1^\circ$  grid for daily and monthly means for July 1983 through December 2004. These fluxes are computed by use of a number of data products. Cloud properties are derived from ISCCP pixel level (DX) data. Temperature and humidity profiles come from the

Goddard Earth Observing System (GEOS-4) reanalysis product of Goddard Space Flight Center. This most recent release uses MATCH aerosols and a higher resolution coastline. Although the algorithms have undergone several improvements, the discrimination of cloud over snow and ice remains a problem with observations currently available.

## 3. Analysis Method

Cloud forcing is defined as the radiation flux for the observed conditions of the sky minus the flux for clear-sky conditions. The SRB data set includes the clear sky flux components computed for each  $1^\circ$  region as well as the fluxes with the observed clouds, so that the cloud forcing is simple to retrieve from the data set. The hypothetical surface temperature that would exist in the absence of clouds is not considered, so that the cloud forcing of upward longwave radiation is taken to be zero.

Monthly mean fluxes were each averaged over the twenty-one-year period of the SRB data set for each calendar month to form the flux components for a climatological average month, and the cloud forcing for each component was computed. The cloud forcing for each component  $R$  is then written as

$$CF_R(x,t) = CF_{RAV}(x) + \sum PC_i(t) EOF_i(x)$$

where  $t$  denotes the month and  $x$  the latitude and longitude of the region,  $CF_{RAV}(x)$  is the annual average of  $R$  for region  $x$ ,  $PC_i(t)$  is the  $i$ -th principal component and  $EOF_i(x)$  is the  $i$ -th empirical orthogonal function (EOF). The principal component thus describes a time history and the EOF is the corresponding geographical distribution

## 4. Results

The annual-mean cloud forcings are considered first and then the annual cycles of the cloud forcing.

The global-average annual-mean of DSW is  $184 \text{ Wm}^{-2}$ , so that the cloud forcing of DSW is  $-59 \text{ Wm}^{-2}$ , i.e. the effect of clouds

is to reduce surface DSW. Figure 1a is a map of annual mean downward shortwave DSW cloud forcing.

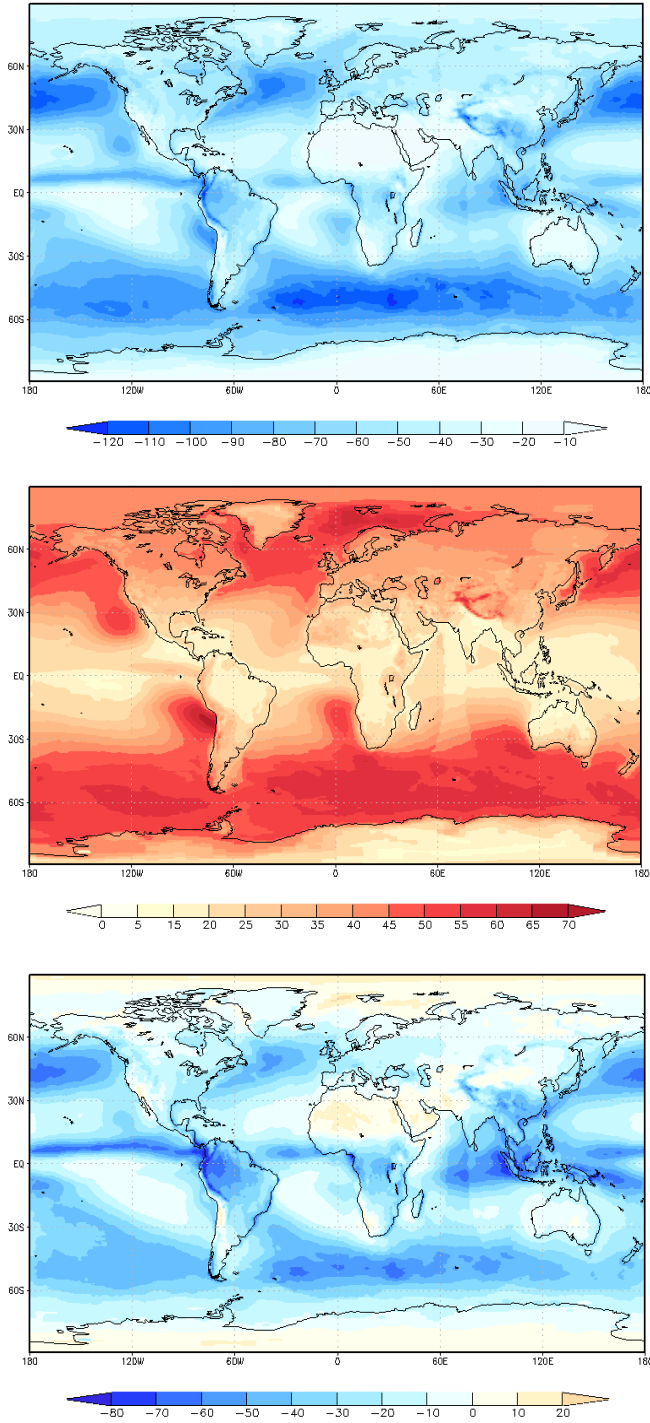


Figure 1: (a) Map of the annual mean of cloud forcing of downward surface shortwave flux (b) Same for downward longwave flux. (c) Same for downward total flux. ( $Wm^{-2}$ )

The downward longwave radiation flux for all-sky conditions global-average annual-mean radiation flux is  $349 Wm^{-2}$ , so that the cloud forcing of DLW is  $34 Wm^{-2}$ . Figure 1b shows the annual-mean downward longwave DLW cloud forcing. The map of annual-mean net total cloud forcing is shown by fig. 1c and is very similar to that for DSW in fig. 1a.

The root-mean-square (RMS) of shortwave cloud forcing at the surface is listed in table 1 and is  $24.7 Wm^{-2}$ . This may be compared with the RMS of the annual cycle of downward shortwave radiative flux at the surface for all sky conditions (Wilber et al., 2006), which is  $60.6 Wm^{-2}$ . The eigenvalues are normalized so as to sum to one and are listed in table 1 also.

Table 1: RMS and eigenvalues for cloud forcing.

	SW CF	LW CF	Total CF
RMS, $Wm^{-2}$	24.7	3.87	25.0
$\lambda_1$	0.880	0.710	0.901
$\lambda_2$	0.063	0.154	0.048
$\lambda_3$	0.028	0.067	0.027
$\lambda_4$	0.015	0.029	0.004
Sum of first 4 e-values	0.986	0.960	0.980

Figure 2 shows the first three principal components of shortwave cloud forcing. The first principal component is very nearly a sine and is an annual cycle with amplitude of  $35 Wm^{-2}$ . The maximum is in June and the minimum is in December, so that it is in phase with the insolation. The first principal component for all-sky DSW has amplitude of  $80 Wm^{-2}$ .

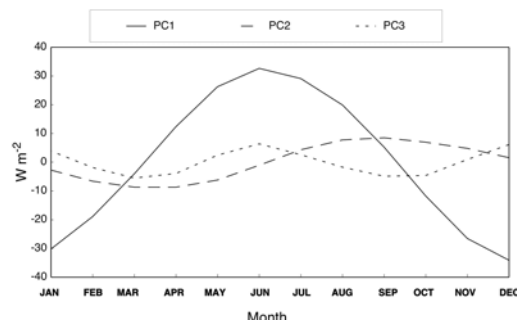


Figure 2: Principal components for downward shortwave flux at surface,  $Wm^{-2}$ .

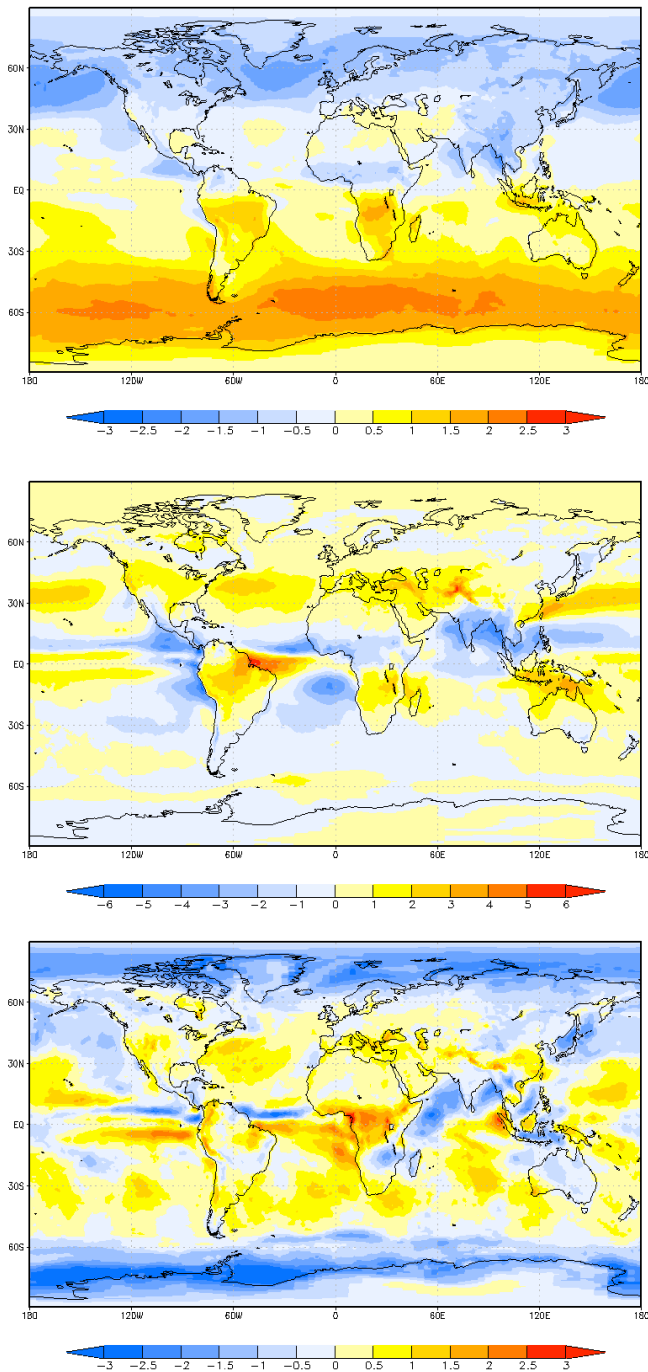


Figure 3: Maps of empirical orthogonal functions for downward shortwave flux at surface, dimensionless. a. EOF-1, b. EOF-2, c. EOF-3.

Figure 3a shows EOF-1, which is the geographical distribution of the DSW cloud forcing corresponding to the first principal component. The EOFs are normalized with a RMS of unity and are measured as standard deviations.

Figure 4 shows the zonal mean of EOF-1 for DSW cloud forcing as a function of latitude. The zonal mean has extrema at 60° north and south latitudes. The maximum in the Southern Hemisphere is 2 standard deviations, whereas in the Northern Hemisphere the extreme value is only -1 because of the land-sea differences.

Figure 4 shows that the zonal mean of EOF-2 for DSW cloud forcing is small except for the local maximum and minimum beside the Equator due to the ITCZ movements and the maximum near 40° N.

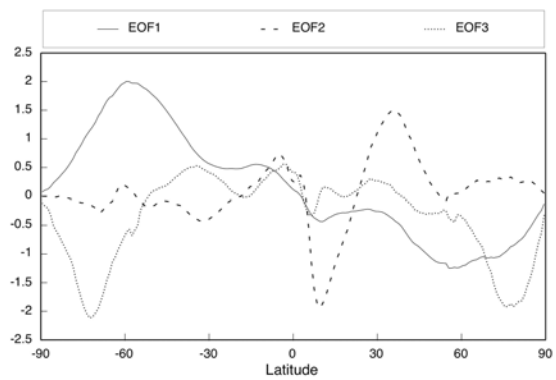


Figure 4: Zonal means of empirical orthogonal functions for downward shortwave flux at surface as functions of latitude, dimensionless.

The third principal component describes 2.8% of the variance and is a semiannual cycle of about  $4 \text{ W}\cdot\text{m}^{-2}$  with maxima in June and December. Figure 3c shows EOF-3 for DSW cloud forcing is largest near the poles due to the semi-annual cycle of insolation. Figure 4 shows that the zonal mean of EOF-3 is small except for the near-polar extrema.

The RMS for downward longwave DLW cloud forcing is  $3.87 \text{ W}\cdot\text{m}^{-2}$ , smaller than the DSW cloud forcing by a factor of 6. The first eigenvalue, 0.710, is smaller and the remaining eigenvalues are larger than for DSW cloud forcing, indicating greater variety of the DLW than the DSW case.

Figure 5 shows that the first principal component for DLW cloud forcing is an



annual cycle with a maximum in August and amplitude of 4 to 5  $\text{Wm}^{-2}$ . The shape is close to a sine, but has a flatter decrease from September to December than a sine wave. Whereas the first principal component of DSW cloud forcing is in phase with the insolation, the DLW cloud forcing lags insolation by two months. This variation of DLW cloud forcing could be due to changes of cloud amount or of cloud base height.

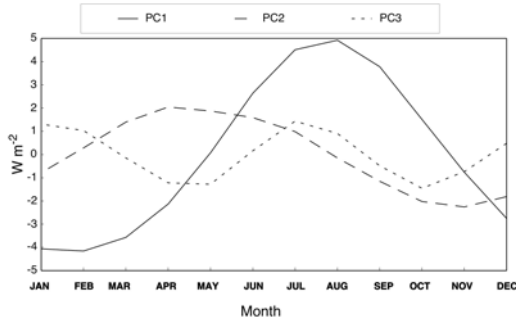


Figure 5: Principal components for downward longwave flux at surface,  $\text{Wm}^{-2}$ .

Figure 6a is the map of EOF-1 for DLW cloud forcing.

Figure 7 shows the zonal means of the first three EOFs of DLW cloud forcing as a function of latitude. The zonal mean of these two bands are 1.3 standard deviations at  $30^\circ\text{S}$  and -2 standard deviations at  $35^\circ\text{N}$ , or 4.2 and  $-6.5 \text{ Wm}^{-2}$  respectively.

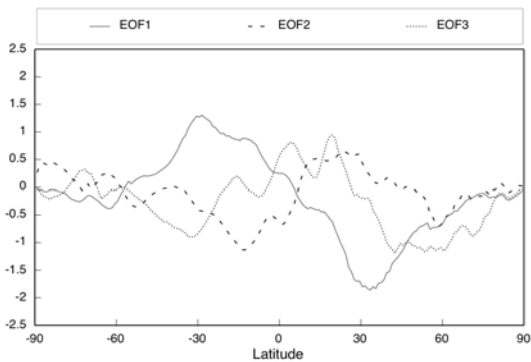


Figure 7: Zonal means of empirical orthogonal functions for downward longwave flux at surface as functions of latitude, dimensionless.

Figure 6b shows EOF-2 for DLW cloud forcing.

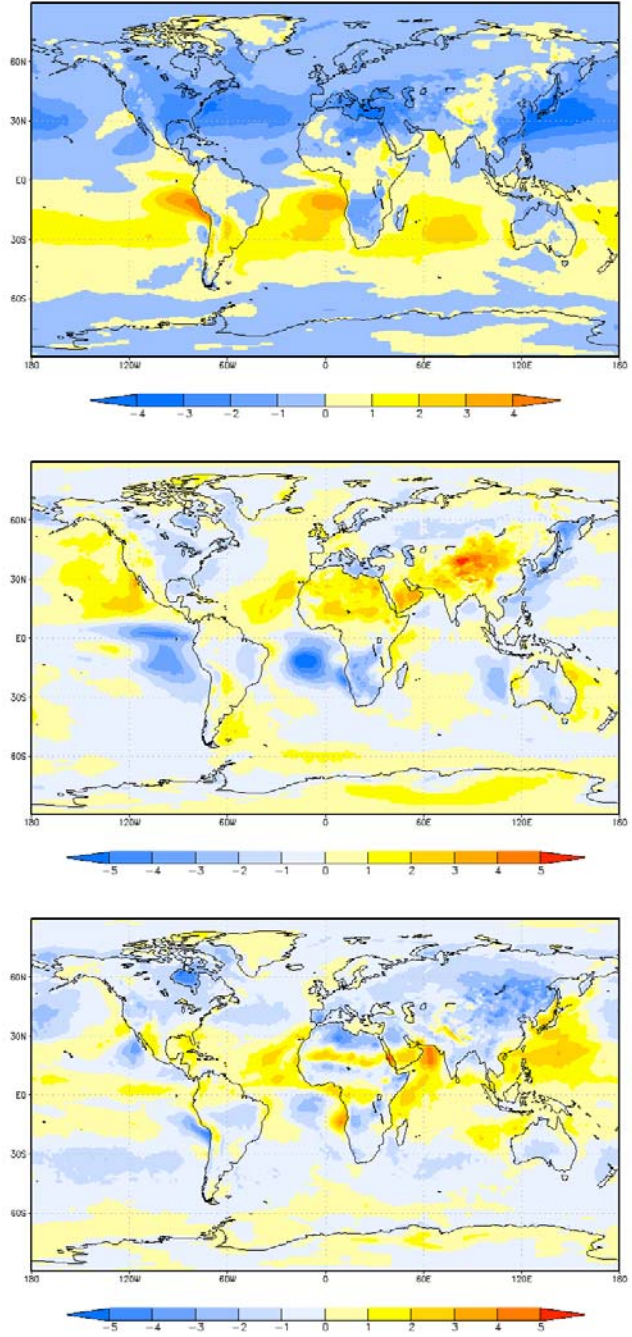


Figure 6: Maps of empirical orthogonal functions for downward longwave flux at surface, dimensionless. a. EOF-1, b. EOF-2, c. EOF-3.

Table 1 shows that the RMS for total downward radiative cloud forcing is  $25.0 \text{ Wm}^{-2}$ , slightly greater than for DSW cloud forcing. The first four eigenvalues for net total cloud forcing are close to those for DSW cloud forcing. Plots of the first three

principal components are indistinguishable from those for DSW cloud forcing and are not shown. Likewise, the maps of the first two EOFs for net total cloud forcing are indistinguishable from those for DSW cloud forcing and the EOF-3 differ only in small details. The close similarity of the net total cloud forcing with the DSW cloud forcing is due to the small RMS of DLW cloud forcing relative to that of DSW cloud forcing. In order to get the energetics of the surface accurately in a circulation model, it is more important to get the downward shortwave calculation accurate than the longwave.

## 5. Conclusions

This paper has quantitatively described the annual cycles of surface radiation components. The next step is to investigate the interactions of these radiation fluxes with the other components of the surface-atmosphere system in order to establish the causes and effects of these variations and thus to increase our understanding of weather and climate processes. Another application of these results is comparison with the output of circulation models, so as to validate or improve the ability of these models to simulate weather and climate processes.

Averaged over the Earth for one year, clouds reduce the insolation at the surface by  $59 \text{ Wm}^{-2}$  and increase the downward longwave radiation flux by  $34 \text{ Wm}^{-2}$ . In order to describe the annual cycles, a principal component analysis is used. The root-mean-square of the annual cycle of cloud forcing of downward shortwave radiation is  $25 \text{ Wm}^{-2}$  and of downward longwave radiation is  $3.9 \text{ Wm}^{-2}$ . Most of the cloud forcing of downward shortwave radiation is in phase with insolation, but the downward longwave radiation lags by two months.

*Acknowledgements:* This work was supported by the Clouds and Earth Radiant Energy System (CERES) program and the Surface Radiation Budget Program of the Earth Science Enterprise of NASA through Langley Research Center by contract to Analytical Sciences and Materials, Inc. and

the National Institute of Aerospace. Data were provided by the Langley Atmospheric Sciences Data Center.

## REFERENCES

- Barkstrom, B. R. and G. L. Smith, 1986: The Earth Radiation Budget Experiment: Science and Implementation, *Rev. of Geophys.*, 24, 379-390.
- Cox, S. J., P. W. Stackhouse, Jr., S. K. Gupta, J. C. Mikovitz, T. Zhang, L. M. Hinkelman, M. Wild, and A. Ohmura 2006: The NASA/GEWEX Surface Radiation Budget project: overview and analysis, *12th Conference on Atmospheric Radiation*, 10-14 July, Madison, WI, Amer. Meteor. Soc. 10.1
- Darnell, W. L., W. F. Staylor, S. K. Gupta, N. A. Ritchey and A. C. Wilber 1992: Seasonal variation of surface radiation budget derived from ISCCP-C1 data, *J. Geophys. Res.* 97, 15741- 15760.
- Gupta, S. K., P. W. Stackhouse., S. J. Cox, J. C. Mikovitz and M. Chiacchio 2004: The NASA/GEWEX Surface Radiation Budget Data *Proc. 13-th Conf. Sat. Met. and Oceanogr.* 20-23 September, Norfolk VA, Amer. Meteor. Soc., P6.6.
- Gupta, S. K., N. A. Ritchey, A. C. Wilber, C. H. Whitlock, G. G. Gibson, and P. W. Stackhouse. 1999: A Climatology of Surface Radiation Budget Derived from Satellite Data., *J. Climate*, 12, 2691-2710.
- Gupta, S. K., W. F. Staylor, W. L. Darnell, A. C. Wilber and N. A. Ritchey, 1993: Seasonal variation of surface and atmospheric cloud radiative forcing over the globe derived from satellite data, *J. Geophys. Res.* 98, 20,761-20,778.
- Harrison, E. F., P. Minnis, B. R. Barkstrom, V. Ramanathan, R. D. Cess, and G. G. Gibson, 1990: Seasonal variation of cloud radiative forcing derived from the Earth Radiation Budget Experiment. *J. Geophys. Res.*, 95, 18687-18703.
- Ramanathan, V., 1987: The role of Earth radiation budget studies in climate and general circulation research, *J. Geophys. Res.*, 92, 4075-4095.

- Ramanathan, V., E. F. Harrison and B. R. Barkstrom, 1989: Climate and the Earth's radiation budget, *Physics Today*, 42, 22-33.
- Rossow, W.B. and R.A. Schiffer, 1991: ISSCP cloud data products, *Bull Amer Met Soc.*, 72, 2-20.
- Schiffer, R. A. and W. B. Rossow, 1983: The International Satellite Cloud Climatology Project (ISCCP): The first project of the World Climate Research Programme, *Bull. Am. Meteorol. Soc.*, 64, 779-784.
- Stackhouse, P. W., S. K. Gupta, S. J. Cox, J. C. Mikovitz, T. Zhang and M. Chiacchio, 2004: Twelve-year surface radiation budget data set, *GEWEX News*, 14, no. 4, 10-12.
- Whitlock, C. H., T. P. Charlock, W. F. Staylor, R. T. Pinker, I. Lazlo, A. Ohmura, H. Gilgen, T. Konzelmann, R. C. DiPasquale, C. D. Moats, S. R. Lecroy, and N. A. Ritchie, 1995: First global WCRP surface radiation budget data set. *Bull. Amer. Met. Soc.*, 76, 905-
- Wilber, A. C., G. L. Smith, S. K. Gupta and P. W. Stackhouse, 2006: Annual cycle of surface shortwave radiation, *J. Climate*, 19, 535-547.